Progress In Electromagnetics Research M, Vol. 43, 39–50, 2015

JRDF Algorithm for Joint Range-DOA-Frequency Estimation of Mixed Near-Field and Far-Field Sources

Fulai Liu[1, 2, *], Jian Ma[1, 2], and Ruiyan Du[1, 2]

Abstract—This paper presents an effective joint range-DOA-frequency (JRDF) estimation method based on fourth-order cumulants for multiple mixed near-field sources and far-field sources impinging on a symmetric uniform linear array, named as JRDF algorithm. Making use of the proposed method, range-DOA-frequency can be effectively estimated by the same eigen-pair of a defined "information matrix" constructed by two fourth-order cumulant matrices. Compared with the related works, the proposed method can provide superior performance, such as higher estimation accuracy, without the procedure of parameter search or parameter matching. Simulation results are presented to demonstrate the efficacy of the proposed approach.

1. INTRODUCTION

Source localization from noisy observations is one of the fundamental problems in array signal processing, such as sonar, radar, seismic exploration system and microphone arrays [1]. Therefore, it has received a significant amount of attention, and a number of algorithms have been developed to deal with far-field sources (FFSs) [2–5] or near-field sources (NFSs) [6–9]. For FFSs (beyond Fresnel zone) scenario, the wavefronts are usually approximated as planar, thus only DOA parameter needs to be estimated when the carrier frequency is known. Otherwise, for the NFSs (in Fresnel zone), as the wavefronts are spherical, both DOA and range parameters should be estimated when the carrier frequency is known as a priori. In some practical applications, the signals received at an array may be the mixture of NFSs and FFSs, for example, when using microphone arrays to localize speakers' localizations, each speaker may be in near-field (NF) or far-field (FF) since speakers' positions keep changing. So the pure NF source localization and pure FF source localization algorithm may encounter problems in localizing mixed NFSs and FFSs.

Recently, several high resolution methods have been presented to resolve the parameter estimation problem for the mixed NFSs and FFSs [10–17]. A two-stage MUSIC algorithm using cumulant is presented to solve the mixed source localization [10]. Despite its effectiveness, this algorithm has a high computational burden since it involves multiple eigenvalue decompositions for high order cumulant matrices and one-dimensional (1-D) MUSIC spectrum peak search. To decrease its computational burden, an efficient application of MUSIC algorithm based on second order statics is proposed in [11]. It requires neither a multidimensional search nor high-order statics. Unfortunately, this method has loss of array aperture. Via ESPRIT-Like and polynomial rooting methods, an effective mixed sources localization algorithm is given in [12]. It can obtain better estimation performance and lower computational cost. A two-stage matrix differencing algorithm is derived to classify and locate mixed NF and FF sources [13]. This method not only improves estimation accuracy, but also achieves a more reasonable classification of the signal types. Du et al. present a space-time matrix to localize mixed

Received 18 May 2015, Accepted 23 July 2015, Scheduled 9 August 2015

* Corresponding author: Fulai Liu (fulailiu@126.com).

[1] Engineer Optimization & Smart Antenna Institute, Northeastern University at Qinhuangdao, China. [2] School of Information Science and Engineering, Northeastern University, Shenyang, China.

NFSs and FFSs [14]. By using this method, both the DOAs and ranges of sources can be estimated by the same eigen-pair of a defined space-time matrix which avoids parameter matching problems. An improved mixed source localization method based on sparse signal reconstruction is proposed in [15]. This method firstly transforms the time-domain data of array into cumulant domain data to estimate DOAs, then constructs the mixed overcomplete basis to get the sparse representation of the array output for range estimation. It can resolve the closely spaced source and provide higher estimation accuracy. A mixed-order MUSIC algorithm for NF and FF sources localization using a sparse symmetric array is proposed in [16]. This method constructs a cumulant matrix to estimate DOAs of the mixed sources by exploiting the special array geometry. Via a crossed array, a three-dimensional (3-D) mixed NF and FF sources localization algorithm is presented in [17]. As it is based on second order statistics and requires 1-D search, it has low computational burden. In addition, it is able to avoid parameter pairing procedure as well.

To decrease the computational burden and avoid parameters pairing, a JRDF estimation algorithm is proposed to resolve the mixed source localization problem when NFSs and FFSs coexist. The ranges, DOAs and frequencies of all incoming signal sources can be estimated by the eigen-pair of a defined "information matrix" based on fourth-order cumulants. The outline of this paper is organized as follows. Section 2 briefly introduces data model. The JRDF estimation algorithm is described in Section 3. Section 4 shows several simulation results to verify the performance of the proposed approach. Finally, Section 5 provides a concluding remark to summarize the paper.

2. DATA MODEL

Consider the receiving system with uniform linear array (ULA) (shown in Fig. 1) which consists of $2N+1$ isotropic sensors. Assume that there are L independent narrowband sources impinging on the ULA from NF or FF.

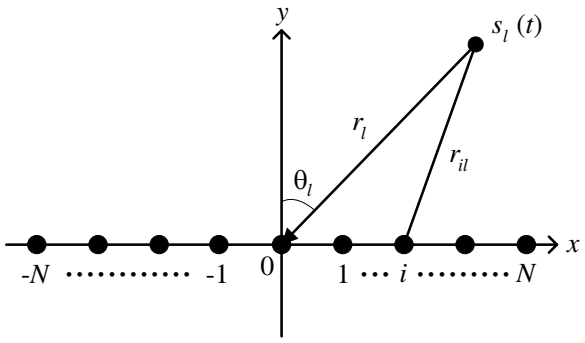

Figure 1. Uniform linear array configuration.

Employ the centre of the array as the phase reference point. Assume that there are L narrowband sources of interest, with complex baseband representations $s_l(t)$, for $l = 1, 2, \ldots, L$. Suppose that the lth source has a carrier frequency of f_l. The signal received at the ith antenna is

$$x_i(t) = \sum_{l=1}^{L} s_l(t) e^{j2\pi f_l t} e^{j\tau_{il}} + n_i(t) \quad (-N \le i \le N) \tag{1}$$

where $x_i(t)$ and $n_i(t)$ denote the output and the additive noise output of the ith sensor.

As θ_l and r_l are the DOA and range of the lth source relative to the phase reference point, respectively, the distance r_{il} from the lth source to the ith sensor is given by a simple application of the law of cosines

$$r_{il} = \sqrt{r_l^2 + (id)^2 - 2 r_l i d \cos\left(\frac{\pi}{2} - \theta_l\right)} \quad -N \le i \le N \tag{2}$$

where d denotes the distance between two adjancent sensors.

The delay τ_{il}, which is associate with the lth source signal propagation time between the phase reference point and the ith sensor, can be expressed as

$$\tau_{il} = \frac{2\pi(r_{il} - r_l)}{\lambda_l} \tag{3}$$

thus using the Fresnel approximation [18], (3) can be approximated as

$$\hat{\tau}_{il} \approx i\frac{-2\pi d}{\lambda_l}\sin(\theta_l) + i^2\frac{\pi d^2}{\lambda_l r_l}\cos^2(\theta_l) \tag{4}$$

For NFSs, r_l is restricted to the Fresnel zone. They must be characterized by both the azimuth DOA and range, because the wavefronts are spherical. For FFSs, r_l is far beyond the Fresnel zone, so we can treat spherical wavefronts as planar wavefronts (plane-wave approximation) when they propagate across the array. When this approximation is substituted into (4), the phase of the delay term becomes a linear function as follows

$$\hat{\tau}_{il} \approx i\frac{-2\pi d}{\lambda_l}\sin(\theta_l) \tag{5}$$

Therefore, FF can be regarded as a special case of the NF.

In addition, the parameters γ_l and ϕ_l are the functions of the azimuth θ_l and range r_l of the lth source

$$\gamma_l = -\frac{2\pi d}{\lambda_l}\sin(\theta_l) \tag{6}$$

and

$$\phi_l = \frac{\pi d^2}{\lambda_l r_l}\cos^2(\theta_l) \tag{7}$$

where $\theta_l \in [-\pi/2, \pi/2]$, $r_l \in [0.62(D^2/\lambda_l)^{1/2}, +\infty)$, D represents the array aperture.

After being sampled with a proper rate f_s that satisfies the Nyquist rate, the data sample $\mathbf{X}(k)$ at the receiver is

$$\mathbf{X}(k) = \mathbf{A}\mathbf{S}(k) + \mathbf{N}(k) \quad (k = 1, 2, \ldots, K) \tag{8}$$

where $\mathbf{X}(k) = [\mathbf{x}_{-N}(k), \ldots, \mathbf{x}_0(k), \ldots, \mathbf{x}_N(k)]^T$ is the array output matrix. $\mathbf{S}(k) = [s_1(k)e^{j\omega_1 k}, s_2(k)e^{j\omega_2 k}, \ldots, s_L(k)e^{j\omega_L k}]^T$ represents the signal waveform vector. The normalized radian frequency $\omega_l = \frac{2\pi f_l}{f_s}$. $\lambda_l = \frac{c}{f_l} = \frac{2\pi c}{\omega_l f_s}$. $\mathbf{N}(k) = [n_{-N}(k), \ldots, n_0(k), \ldots, n_{+N}(k)]^T$ stands for the noise vector. K stands for the snapshot number. $\mathbf{A} = [\mathbf{a}(\theta_1, r_1), \mathbf{a}(\theta_2, r_2), \ldots, \mathbf{a}(\theta_L, r_L)]$ is the $(2N+1) \times L$ array steering matrix of the mixed NFSs and FFSs. The array steering vector can be given as

$$\mathbf{a}(\theta_l, r_l) = \left[e^{j[(-N)\gamma_l + (-N)^2\phi_l]}, \ldots, e^{j[(-i)\gamma_l + (-i)^2\phi_l]}, \ 1, \ e^{j[i\gamma_l + i^2\phi_l]}, \ldots, e^{j[N\gamma_l + N^2\phi_l]}\right]^T \tag{9}$$

where the superscript $(\cdot)^T$ stands for the matrix transpose. $r_l \in [0.62(D^2/\lambda_l)^{1/2}, 2D^2/\lambda_l] \cup (2D^2/\lambda_l, +\infty)$.

The common assumptions are listed as follows

(A1) The source signals are mutually independent, non-Gaussian, narrowband stationary processes with nonzero kurtosis.

(A2) The sensor noise is zero-mean (white or colored) Gaussian signals and independent of the source signals.

(A3) The array is a ULA with element spacing $d \leqslant \min(\lambda_l/4)$.

(A4) The array is a symmetric array with $2N+1$ sensors and the source number $L < 2N+1$ is assumed.

(A5) The wavelength parameters of the sources are different from each other, that is $\omega_i \neq \omega_j$ for $i \neq j$.

3. ALGORITHM FORMULATION

To develop an efficient joint estimation algorithm, we define a fourth-order cumulant matrix $\mathbf{C}_1$, the (m,n)th element of which is defined as

$$\mathbf{C}_1(m,n) = \mathrm{cum}\left\{\mathbf{x}_0(k), \mathbf{x}_0^*(k), \mathbf{x}_{m-N-1}(k), \mathbf{x}_{n-N-1}^*(k)\right\} \tag{10}$$

where the superscript $(\cdot)^*$ represents the complex conjugate. Substituting (8) into (10) and using the multilinearity property of cumulant together with the assumptions (A1) and (A2), we can get $\mathbf{C}_1$ as follows

$$\begin{aligned}\mathbf{C}_1(m,n) \;=\; & \sum_{l=1}^{L} c_{4,s_l} e^{j\left\{(m-n)\gamma_l + \left[(m-N-1)^2-(n-N-1)^2\right]\phi_l\right\}} = \sum_{l=1}^{L} c_{4,s_l} e^{j\left\{(m-N-1)\gamma_l + (m-N-1)^2\phi_l\right\}} \\ & \times \left(e^{j\left\{(n-N-1)\gamma_l + (n-N-1)^2\phi_l\right\}}\right)^* \quad (m,n \in [1, 2N+1])\end{aligned} \tag{11}$$

where $c_{4,s_l} = \mathrm{cum}\{|s_l(t)|^4\}$ denotes the kurtosis of $s_l(t)$. Let $\mathbf{C}_{4s} = \mathrm{diag}\{c_{4,s_1}, c_{4,s_2}, \ldots, c_{4,s_L}\}$ be a diagonal matrix composed of the source kurtosis, thus we have

$$\mathbf{C}_1 \;=\; \mathbf{B}\mathbf{C}_{4s}\mathbf{B}^H \tag{12}$$

$$\mathbf{B} \;=\; [\mathbf{b}(\gamma_1), \mathbf{b}(\gamma_2), \ldots, \mathbf{b}(\gamma_l), \ldots, \mathbf{b}(\gamma_L)] \tag{13}$$

$$\mathbf{b}(\gamma_l) \;=\; \left[e^{j[(-N)\gamma_l + (-N)^2\phi_l]}, \ldots, 1, \ldots, e^{j[N\gamma_l + N^2\phi_l]}\right]^T \quad (l = 1, \ldots, L) \tag{14}$$

where the superscript $(\cdot)^H$ denotes Hermitian transpose.

Since all source signals are assumed to have nonzero kurtosis, $\mathbf{C}_{4s}$ is an invertible diagonal matrix. Additionally, $\mathrm{rank}(\mathbf{B}) = L$, hence, $\mathbf{C}_1$ is a $(2N+1) \times (2N+1)$ matrix with rank L.

Furthermore, for different sensor lags, we define

$$\mathbf{C}_2(m,n) = \mathrm{cum}\left\{\mathbf{x}_0(k+1), \mathbf{x}_0^*(k), \mathbf{x}_{m-N-1}(k), \mathbf{x}_{n-N-1}^*(k)\right\} \quad (m,n \in [1, 2N+1]) \tag{15}$$

and under the narrow-band assumption, we have $s_l(k+1) \approx s_l(k)$.

Similar to (12), $\mathbf{C}_2$ has the following expression

$$\mathbf{C}_2 = \mathbf{B}\mathbf{\Omega}\mathbf{C}_{4s}\mathbf{B}^H \tag{16}$$

and

$$\mathbf{\Omega} = \mathrm{diag}\left\{e^{j\omega_1}, e^{j\omega_2}, \ldots, e^{j\omega_L}\right\} \tag{17}$$

It is easy to know that $\mathbf{C}_2$ is also a $(2N+1) \times (2N+1)$ matrix with rank L.

Let $\mathbf{P} = \mathrm{diag}\{\rho_1, \rho_2, \ldots, \rho_{2N+1}\}$ and $\mathbf{V} = [\mathbf{v}_1, \mathbf{v}_2, \ldots, \mathbf{v}_{2N+1}]$ be the eigenvalues and the corresponding eigenvectors of $\mathbf{C}_1$, then we can get

$$\mathbf{C}_1 = \sum_{l=1}^{2N+1} \rho_l \mathbf{v}_l \mathbf{v}_l^H = \mathbf{V}\mathbf{P}\mathbf{V}^H = \mathbf{V}_s\mathbf{P}_s\mathbf{V}_s^H + \mathbf{V}_n\mathbf{P}_n\mathbf{V}_n^H \tag{18}$$

where $\mathbf{P} = \mathrm{diag}\{\rho_1, \rho_2, \ldots, \rho_{2N+1}\}$ with $\rho_1 \geq \rho_2 \geq \ldots \geq \rho_L > \rho_{L+1} = \ldots = \rho_{2N+1} = 0$. $\mathbf{V} = [\mathbf{V}_s\mathbf{V}_n]$. $\mathbf{V}_s = [\mathbf{v}_1, \mathbf{v}_2, \ldots, \mathbf{v}_L]$, $\mathbf{P}_s = \mathrm{diag}\{\rho_1, \rho_2, \ldots, \rho_L\}$, $\mathbf{V}_n = [\mathbf{v}_{L+1}, \mathbf{v}_{L+2}, \ldots, \mathbf{v}_{2N+1}]$ and $\mathbf{P}_n = \mathrm{diag}\{\rho_{L+1}, \rho_{L+2}, \ldots, \rho_{2N+1}\}$.

Similarly, define $\mathbf{C}_3$ as follows

$$\mathbf{C}_3 = \sum_{l=1}^{L} \frac{1}{\rho_l} \mathbf{v}_l \mathbf{v}_l^H = \mathbf{V}_s {\mathbf{P}_s}^{-1} \mathbf{V}_s^H \tag{19}$$

From (12) and (18), it is easy to know that the signal subspace $\mathbf{V}_s$ concides with the range space of $\mathbf{B}$. Since $\mathrm{span}\{\mathbf{V}_s\} = \mathrm{span}\{\mathbf{B}\}$, there must exist a unique invertible matrix $\mathbf{T}$, such that $\mathbf{B} = \mathbf{V}_s\mathbf{T}$. Therefore, it holds that

$$\mathbf{V}_s\mathbf{V}_s^H\mathbf{B} = \mathbf{V}_s\mathbf{V}_s^H\mathbf{V}_s\mathbf{T} = \mathbf{V}_s\mathbf{T} = \mathbf{B} \tag{20}$$

Making use of $\mathbf{C}_2$ and $\mathbf{C}_3$, define an "information matrix" $\mathbf{C}$ (which includes the information of DOAs, ranges and frequencies) as following

$$\mathbf{C} = \mathbf{C}_2\mathbf{C}_3 \tag{21}$$

Then we have the following Theorem.

Theorem 3.1. Assume that there are L (near-field or far-field) narrow-band sources, with the complex baseband representations $s_l(t)(1 \le l \le L)$ such that the lth source has a carrier frequency f_l and arrives a ULA from direction θ_l, range r_l. If there are no same elements on the diagonal of matrix $\mathbf{\Omega}$, then, the L largest nonzero eigenvalues of $\mathbf{C}$ are equal to the L elements on the diagonal of matrix $\mathbf{\Omega}$, and the corresponding eigenvectors are equal to the corresponding column vectors of $\mathbf{B}$, namely $\mathbf{CB} = \mathbf{B\Omega}$.

Proof: Under the above assumption, it is easy to know that $\mathbf{B}$ is a full rank matrix. Furthermore, we draw a conclusion that $\mathrm{rank}(\mathbf{B}) = \mathrm{rank}(\mathbf{C}) = L$. From (12), (16) and (18)$\sim$(20), the following equation can be obtained

$$\begin{aligned}\mathbf{CB} &= \mathbf{C}_2\mathbf{C}_3\mathbf{B} = \mathbf{B\Omega}\mathbf{C}_{4s}\mathbf{B}^H\mathbf{V}_s\mathbf{P}_s^{-1}\mathbf{V}_s^H\mathbf{B} = \mathbf{B\Omega}\left(\mathbf{B}^H\mathbf{B}\right)^{-1}\mathbf{B}^H\left(\mathbf{B}\mathbf{C}_{4s}\mathbf{B}^H\right)\mathbf{V}_s\mathbf{P}_s^{-1}\mathbf{V}_s^H\mathbf{B} \\ &= \mathbf{B\Omega}\left(\mathbf{B}^H\mathbf{B}\right)^{-1}\mathbf{B}^H\mathbf{C}_1\mathbf{V}_s\mathbf{P}_s^{-1}\mathbf{V}_s^H\mathbf{B} = \mathbf{B\Omega}\left(\mathbf{B}^H\mathbf{B}\right)^{-1}\mathbf{B}^H\left(\mathbf{V}_s\mathbf{P}_s\mathbf{V}_s^H\right)\mathbf{V}_s\mathbf{P}_s^{-1}\mathbf{V}_s^H\mathbf{B} \\ &= \mathbf{B\Omega}\left(\mathbf{B}^H\mathbf{B}\right)^{-1}\mathbf{B}^H\mathbf{V}_s\mathbf{V}_s^H\mathbf{B} = \mathbf{B\Omega}\left(\mathbf{B}^H\mathbf{B}\right)^{-1}\mathbf{B}^H\mathbf{B} = \mathbf{B\Omega}\end{aligned} \tag{22}$$

where the superscript $(\cdot)^{-1}$ denotes matrix inverse.

This concludes the proof.

Remarks:

(1) From Theorem 3.1, it can be easily seen that the array response matrix $\mathbf{B}$ and the diagonal matrix $\mathbf{\Omega}$ can be obtained by computing the eigendecomposition of the "information matrix" $\mathbf{C}$. The following incoming angle θ_l, range r_l and frequency f_l can be estimated by making use of the lth eigenpair of the matrix $\mathbf{C}$, that is, the paring of the estimated 3-D parameters is automatically determined.

(2) If there are several sources close in the angle of incidence θ or range r, but there are no same elements on the diagonal of matrix $\mathbf{\Omega}$, then Theorem 3.1 is still true, namely, it can resolve the incoming rays with very close angles or very close ranges under the aforementioned conditional restriction.

Meanwhile, $\mathbf{C}$ can be decomposed into

$$\mathbf{C} = \sum_{l=1}^{2N+1}\alpha_l\mathbf{u}_l\mathbf{u}_l^H = \mathbf{U\Lambda}\mathbf{U}^H = \mathbf{U}_s\mathbf{\Lambda}_s\mathbf{U}_s^H + \mathbf{U}_n\mathbf{\Lambda}_n\mathbf{U}_n^H \tag{23}$$

where $\mathbf{\Lambda} = \mathrm{diag}\{\alpha_1, \alpha_2, \ldots, \alpha_{2N+1}\}$ with $\alpha_1 \ge \alpha_2 \ge \ldots \ge \alpha_L > \alpha_{L+1} = \ldots = \alpha_{2N+1} = 0$. $\mathbf{U} = [\mathbf{U}_s\mathbf{U}_n]$. $\mathbf{U}_s = [\mathbf{u}_1, \mathbf{u}_2, \ldots, \mathbf{u}_L]$, $\mathbf{\Lambda}_s = \mathrm{diag}\{\alpha_1, \alpha_2, \ldots, \alpha_L\}$, $\mathbf{U}_n = [\mathbf{u}_{L+1}, \mathbf{u}_{L+2}, \ldots, \mathbf{u}_{2N+1}]$ and $\mathbf{\Lambda}_n = \mathrm{diag}\{\alpha_{L+1}, \alpha_{L+2}, \ldots, \alpha_{2N+1}\}$.

From (23), it is easy to see that $e^{j\omega_l}$ and $\mathbf{b}(\gamma_l)$ $(l = 1, 2, \ldots, L)$ are just the eigenvalue and corresponding eigenvector of $\mathbf{C}$. Based on (13), (14), (22) and (23), f_l and $\mathbf{b}(\gamma_l)$ can be given by

$$f_l = \frac{\mathrm{angle}(\alpha_l)f_s}{2\pi} \tag{24}$$

and

$$\mathbf{b}(\gamma_l) = \frac{\mathbf{u}_l}{\mathbf{u}_l[N+1]} \tag{25}$$

where the angle$(\cdot)$ denotes the phase angle operator.

To facilitate the representation, let $\mathbf{b}_l$ take the place of $\mathbf{b}(\gamma_l)$ and the ith element of $\mathbf{b}_l$ can be expressed as $\mathbf{b}_l(i)$, thus from (13) and (14), it has the following form

$$\mathbf{b}_l(i) = e^{j[(-N-1+i)\gamma_l + (-N-1+i)^2\phi_l]} \tag{26}$$

By using (26), $\mathbf{d}_l(i)$ and $\mathbf{e}_l(i)$ have the following expression

$$\begin{aligned}\mathbf{d}_l(i) &= \mathbf{b}_l(i+1)\mathbf{b}_l^*(i)\mathbf{b}_l^*(3)\mathbf{b}_l(2) \\ &= e^{j[(-N+i)\gamma_l + (-N+i)^2\phi_l]}e^{-j[(-N+i-1)\gamma_l + (-N+i-1)^2\phi_l]} \\ &\quad e^{-j[(-N+2)\gamma_l + (-N+2)^2\phi_l]}e^{j[(-N+1)\gamma_l + (-N+1)^2\phi_l]} = e^{j[2(i-2)\phi_l]}\end{aligned} \tag{27}$$

and

$$\begin{aligned}\mathbf{e}_l(i) &= \mathbf{b}_l(i+1)\mathbf{b}_l^*(i)\mathbf{b}_l^*(2N-1)\mathbf{b}_l(2N)\\ &= e^{j[(-N+i)\gamma_l+(-N+i)^2\phi_l]}e^{-j[(-N+i-1)\gamma_l+(-N+i-1)^2\phi_l]}\\ &\quad e^{-j[(N-2)\gamma_l+(N-2)^2\phi_l]}e^{j[(N-1)\gamma_l+(N-1)^2\phi_l]} = e^{j[2(i-2)\phi_l+2\gamma_l]}\end{aligned} \tag{28}$$

Based on $\mathbf{b}_l$, we can form two $2N$-dimensional column vectors as follows

$$\mathbf{d}_l = \begin{bmatrix} \mathbf{b}_l(2)\mathbf{b}_l^*(1)\mathbf{b}_l^*(3)\mathbf{b}_l(2) \\ \mathbf{b}_l(3)\mathbf{b}_l^*(2)\mathbf{b}_l^*(3)\mathbf{b}_l(2) \\ \vdots \\ \mathbf{b}_l(2N-1)\mathbf{b}_l^*(2N-2)\mathbf{b}_l^*(3)\mathbf{b}_l(2) \\ \mathbf{b}_l(2N)\mathbf{b}_l^*(2N-1)\mathbf{b}_l^*(3)\mathbf{b}_l(2) \\ \mathbf{b}_l(2N+1)\mathbf{b}_l^*(2N)\mathbf{b}_l^*(3)\mathbf{b}_l(2) \end{bmatrix} = \begin{bmatrix} e^{j(-2)\phi_l} \\ 1 \\ \vdots \\ e^{j(4N-8)\phi_l} \\ e^{j(4N-6)\phi_l} \\ e^{j(4N-4)\phi_l} \end{bmatrix} \tag{29}$$

and

$$\mathbf{e}_l = \begin{bmatrix} \mathbf{b}_l(2)\mathbf{b}_l^*(1)\mathbf{b}_l^*(2N-1)\mathbf{b}_l(2N) \\ \mathbf{b}_l(3)\mathbf{b}_l^*(2)\mathbf{b}_l^*(2N-1)\mathbf{b}_l(2N) \\ \vdots \\ \mathbf{b}_l(2N-1)\mathbf{b}_l^*(2N-2)\mathbf{b}_l^*(2N-1)\mathbf{b}_l(2N) \\ \mathbf{b}_l(2N)\mathbf{b}_l^*(2N-1)\mathbf{b}_l^*(2N-1)\mathbf{b}_l(2N) \\ \mathbf{b}_l(2N+1)\mathbf{b}_l^*(2N)\mathbf{b}_l^*(2N-1)\mathbf{b}_l(2N) \end{bmatrix} = \begin{bmatrix} e^{j[(-2)\phi_l+2\gamma_l]} \\ e^{j[2\gamma_l]} \\ \vdots \\ e^{j[(4N-8)\phi_l+2\gamma_l]} \\ e^{j[(4N-6)\phi_l+2\gamma_l]} \\ e^{j[(4N-4)\phi_l+2\gamma_l]} \end{bmatrix} \tag{30}$$

Based on $\mathbf{d}_l$ and $\mathbf{e}_l$, $\{\gamma_l, \phi_l\}$ can be given by

$$\gamma_l = \frac{1}{4N}\sum_{i=1}^{2N}\frac{\mathbf{e}_l(i)}{\mathbf{d}_l(i)} \tag{31}$$

and

$$\phi_l = \frac{1}{8N-4}\left[\sum_{i=1}^{2N-1}\arg\left(\frac{\mathbf{d}_l(i+1)}{\mathbf{d}_l(i)}\right) + \sum_{i=1}^{2N-1}\arg\left(\frac{\mathbf{e}_l(i+1)}{\mathbf{e}_l(i)}\right)\right] \tag{32}$$

The wavelength of the lth source λ_l is easily obtained from f_l. According to (6), (7), (31) and (32), the azimuth and range estimation of the lth source can be in turn expressed as

$$\theta_l = \arcsin\left(-\frac{\gamma_l\lambda_l}{2\pi d}\right) \tag{33}$$

and

$$r_l = \frac{\pi d^2}{\lambda_l\phi_l}\cos^2(\theta_l) \tag{34}$$

In fact, according to (34), we can easily determine that the lth source is a NF or FF one. When $r_l \in [0.62(D^2/\lambda_l)^{1/2}, 2D^2/\lambda_l]$ (Fresnel region), we can determine that the lth source corresponding to r_l is a NF source. On the contrary, when $r_l \in (2D^2/\lambda_l, +\infty)$, we can determine that the lth source corresponding to r_l is a FF source.

4. SUMMARY OF JRDF

(1) Collect data and conduct two fourth-order cumulant matrices $\mathbf{C}_1$ and $\mathbf{C}_2$ denoting the estimate $\hat{\mathbf{C}}_1$ and $\hat{\mathbf{C}}_2$, respectively.

(2) Compute the eigendecomposition of $\hat{\mathbf{C}}_1$ and use its L maximum nonzero eigenvalues $\hat{\mathbf{P}}_s = \mathrm{diag}\{\hat{\rho}_1, \ldots, \hat{\rho}_L\}$ and the corresponding eigenvectors $\hat{\mathbf{V}}_s$ to define $\hat{\mathbf{C}}_3$ according to AIC [19], if L is unknown.

(3) Define $\hat{\mathbf{C}}$ by using $\hat{\mathbf{C}}_2$ and $\hat{\mathbf{C}}_3$, then compute the eigendecomposition of $\hat{\mathbf{C}}$.

(4) Use the L maximum nonzero eigenvalues $\hat{\mathbf{\Lambda}}_s$ and its corresponding eigenvectors $\hat{\mathbf{U}}_s$ (the eigenpairs $(\hat{\alpha}_l, \hat{\mathbf{u}}_l), l = 1, 2, \ldots, L$) of $\hat{\mathbf{C}}$ to estimate the frequency of the lth source $\hat{f}_l$ and $\hat{\mathbf{b}}_l$ by (24) and (25), respectively.

(5) Estimate $\hat{\mathbf{d}}_l$ and $\hat{\mathbf{e}}_l$ by making use of $\hat{\mathbf{b}}_l$ from (29) and (30), respectively.

(6) Implement $\hat{\mathbf{d}}_l$ and $\hat{\mathbf{e}}_l$ to estimate $\hat{\gamma}_l$ and $\hat{\phi}_l$ by (31) and (32), respectively.

(7) The DOA and range estimations of the lth source can be in turn expressed as (33) and (34), respectively.

(8) Use the range estimation of the lth source $\hat{r}_l$ to determine whether the lth source is NFS or FFS.

Remarks:

(1) It is well known that the accuracy of the results is concerned with array aperture. When $\tau \ll 1/B$ ($\tau = D/c$ with D denoting the array aperture, c standing for the velocity of electromagnetic waves, B being the incoming signal's bandwidth, respectively), as the array aperture becomes larger, the accuracy of the results gets higher. Moreover, the array aperture is concerned with the number of the array's elements and the distance between two adjacent array elements. As the number of the array's elements and the distance between two adjacent elements become larger, the accuracy of the results grows higher. However, when $d > \lambda/4$ (d is the distance between two adjacent array elements and λ equal to the wavelength), although the accuracy of the results improves, it will cause phase ambiguity. So the distance between two adjacent array elements is set to $d = \lambda/4$.

(2) As the antenna array patterns may not be entirely consistent, it may cause gain-and-phase errors in the real world. In reality, the elements of the array should be calibrated according to the existing calibration methods such as active calibration [20] and self-calibration [21], etc.

(3) The source number estimation problem is an important problem in array signal processing, etc. Generally, the source number estimation is a prior. If the number is unknown, we can use AIC [19] (Akaike Information Criteria) and GDE [22] (Gerschgorin's Disk Estimation) to detect the number of the incoming signals. However, this paper mainly focuses on the joint range-DOA-frequency estimation problem. The source number estimation problem may be beyond the scope of this paper.

5. COMPUTATIONAL COMPLEXITY

We briefly investigate the computational complexity of the proposed algorithm. The computational complexity of the proposed algorithm mainly includes: (1) fourth-order cumulants matrix construction of two $P \times P$ matrixes $\mathbf{C}_1$ and $\mathbf{C}_2$, respectively, of orders $O(9P^2)$ (where $P = 2N + 1$, $Q = 4N + 1$); (2) the eigendecomposition (EVD) of two $P \times P$ matrixes $\mathbf{C}_1$ and $\mathbf{C}$, respectively, of orders $O(4/3P^3)$. Table 1 presents the complexity of the proposed method and the methods in [10]. For comparison, the method in [10] and the proposed method are named as TSMUSIC and JRDF, respectively.

Table 1. Comparison of the computational complexity of the proposed algorithm with TSMUSIC.

Algorithms	construction of matrix	EVD	peak search
JRDF	twice $O(9P^2)$	twice $O(4/3P^3)$	without
TSMUSIC	ones $O(9P^2)$	ones $O(4/3P^3)$	ones
	ones $O(9Q^2)$	ones $O(4/3Q^3)$	

6. SIMULATION RESULTS

In this section, several simulation results are provided to illustrate the performance of JRDF. Consider a ULA composed of 5 sensors with quarter-wavelength spacing. The input signal-to-noise ratio (SNR) is defined as $10\log 10(\sigma_s^2/\sigma_n^2)$, where σ_s^2 denotes the power of signal source and σ_n^2 stands for the noise power. The sampling rate is 20 MHz. Two equal-power, statistically independent narrow-band sources, respectively with center frequency 2.0 and 3.0 MHz (i.e., $\omega_1 = 0.2\pi$ rad/s, $\lambda_1 = 150$, $\omega_2 = 0.3\pi$ rad/s and

$\lambda_2 = 100$), radiate on the array. For comparison, we simultaneously execute the algorithm in [10] and the related CRB [23] (see Appendix for details) in the following experiments and figures. The frequency, DOA and range estimates are scaled in units of MHz, degree and wavelength. Assume that there are one NFS and one FFS and they are located at $(10°, \lambda_1)$ and $(20°, 45\lambda_2)$. The number of snapshots is $N = 100$. And the performance of these algorithms is measured by the estimated root mean-square error (RMSE) of 400 independent Monte Carlo runs. The RMSE_f, RMSE_θ and RMSE_r are defined as follows

$$\begin{cases} \mathrm{RMSE}_f = \sqrt{E\left[\sum_{l=1}^{L}\left(f_l - \hat{f}_l\right)^2\right]} \\ \mathrm{RMSE}_\theta = \sqrt{E\left[\sum_{l=1}^{L}\left(\theta_l - \hat{\theta}_l\right)^2\right]} \\ \mathrm{RMSE}_r = \sqrt{E\left[\sum_{l=1}^{L}\left(r_l - \hat{r}_l\right)^2\right]} \end{cases} \tag{35}$$

where $\hat{f}_l$, $\hat{\theta}_l$ and $\hat{r}_l$ are the estimate of f_l, θ_l and r_l, for $l = 1, 2, \ldots, L$.

Figures 2, 3 and 4 give RMSE_f curves with SNR from -15 to 15 dB. The solid line stands for the RMSE curve of the proposed method. The dotted line represents the RMSE curve of TSMUSIC. The dotted and dash line shows the RMSE curve of the related CRB. Fig. 2 shows that JRDF estimation algorithm has high frequency estimation accuracy. By contrast, TSMUSIC method assumes that the carrier frequency is known as a priori. From Figs. 3 and 4, we can note that the proposed method outperforms TSMUSIC method in frequency, DOA and range estimates. In addition, the proposed method shows a more satisfactory performance than TSMUSIC and the RMSEs are reasonably close to the related CRB.

When SNR is set to 10 dB and the snapshot number varies from 50 to 500, RMSE_f curves of the JRDF and related CRB are shown in Fig. 5. In addition, the RMSE_θ and RMSE_r curves of the aforementioned two algorithms and related CRB are shown in Fig. 6 and Fig. 7, respectively. From Fig. 5, we can know that JRDF estimation algorithm has satisfactory frequency performance. However, TSMUSIC assumes that the carrier frequency is known as a priori. As shown in Fig. 6 and Fig. 7, the proposed method has higher estimation accuracy than that of TSMUSIC, and the curves of the proposed method are closer to the related CRB.

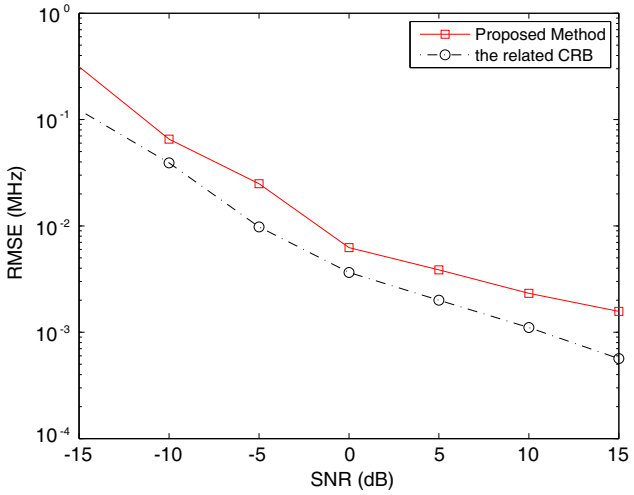

Figure 2. RMSE_f curves versus SNR.

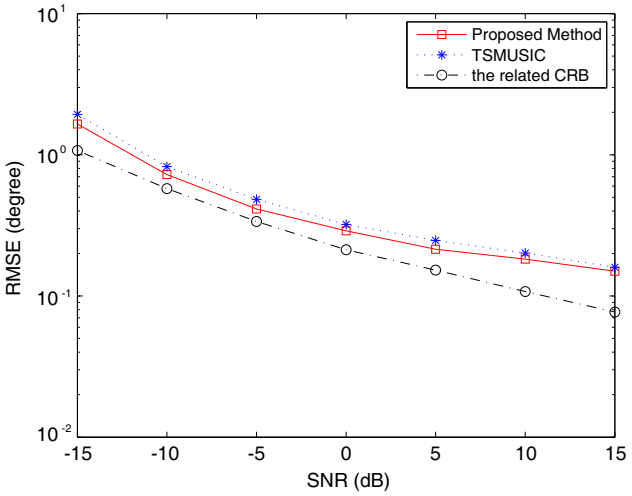

Figure 3. RMSE_θ curves versus SNR.

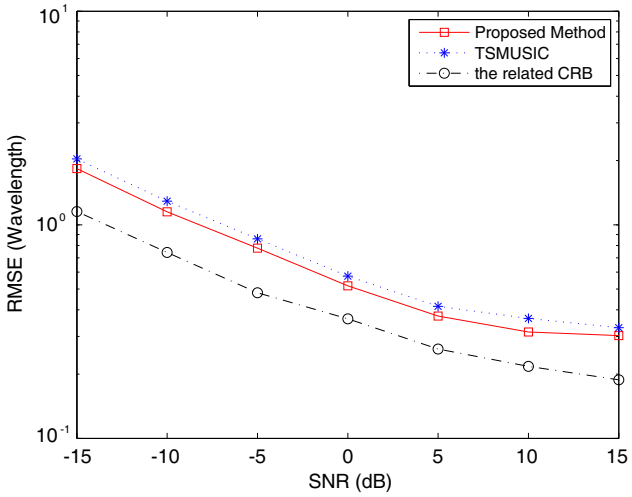

Figure 4. RMSE_r curves versus SNR.

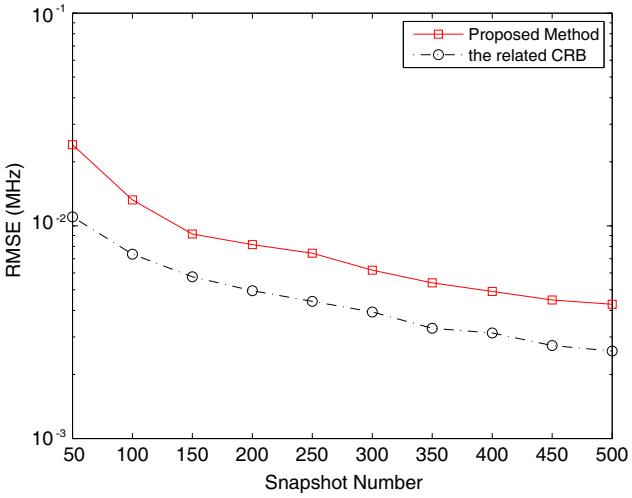

Figure 5. RMSE_f curves versus snapshot number.

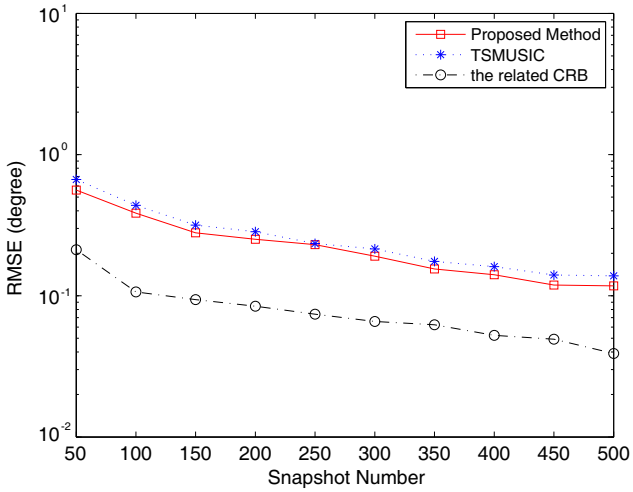

Figure 6. RMSE_θ curves versus snapshot number.

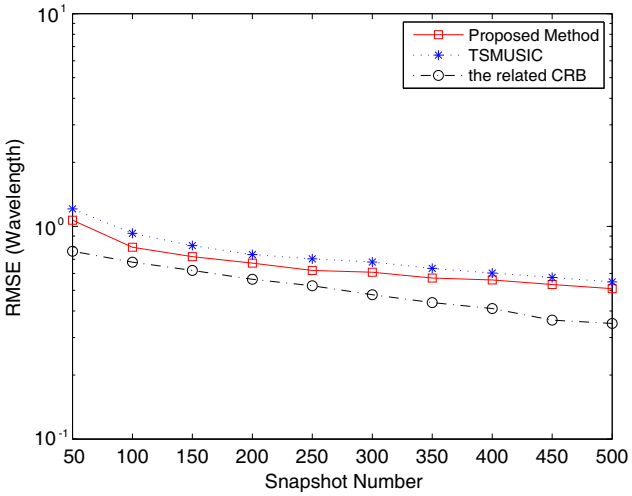

Figure 7. RMSE_r curves versus snapshot number.

7. CONCLUSIONS

In this paper, a JRDF estimation algorithm based on fourth-order cumulants is presented for mixed sources localization. Eigen-pairs of the defined "information matrix" are used to estimate the ranges, DOAs and frequencies. So the pairing of the estimated parameters is automatically determined. The presented approach has a lower computational complexity, but it exhibits superior performance, such as smaller estimation error and better robustness to SNR change.

ACKNOWLEDGMENT

This work has been supported by the Program for New Century Excellent Talents in University (NCET-13-0105), and by the Support Program for Hundreds of Outstanding Innovative Talents in Higher Education Institutions of Hebei Province, under Grant No. BR2-259, and by the Fundamental Research Funds for the Central Universities under Grant No. N142302001, and by the Program for Liaoning Excellent Talents in University (LJQ2012022), and by Directive Plan of Science Research from the

Bureau of Education of Hebei Province, China, under Grant No. Z2011129, and by the National Natural Science Foundation of China under Grant No. 60904035, and by the Specialized Research Fund for the Doctoral Program of Higher Education of China (No. 20130042110003), and by Science and Technology Support Planning Project of Northeastern University at Qinhuangdao (XNK201302). The authors also gratefully acknowledge the helpful comments and suggestions of the reviewers, which have significantly improved the presentation of this paper.

APPENDIX A.

In this appendix, we derive the CRB for the estimated parameters [9].

By virtue of (8), we can get

$$n_i(k) = x_i(k) - \sum_{l=1}^{L} s_l(k) e^{j\omega_l k} e^{j\left(i\gamma_l + i^2\phi_l\right)} \tag{A1}$$

From (A1), we define the probability density function $p(\mathbf{x}|\psi)$ as

$$p(\mathbf{x}|\psi) = \prod_{k=1}^{K}\prod_{i=-N}^{N} \frac{1}{\sqrt{2\pi\sigma^2}} e^{-\frac{1}{2\sigma^2}\left(x_i(k)-\sum\limits_{l=1}^{L} s_l(k)e^{j\omega_l k}e^{j(i\gamma_l+i^2\phi_l)}\right)^H\left(x_i(k)-\sum\limits_{l=1}^{L} s_l(k)e^{j\omega_l k}e^{j(i\gamma_l+i^2\phi_l)}\right)} \tag{A2}$$

where $\mathbf{x} = [\mathbf{x}(1), \mathbf{x}(2), \ldots, \mathbf{x}(K)]^T$ and $\psi = [\psi_1, \ldots, \psi_l, \ldots, \psi_L]^T$. ψ_l can be expressed as follows

$$\psi_l = [\omega_l \ \theta_l \ r_l] \tag{A3}$$

The natural algorithm of $p(\mathbf{x}|\psi)$ can be expressed as

$$\begin{aligned} \ln(p(\mathbf{x}|\psi)) \ = \ & -\frac{1}{2}(2N+1)K\ln\left(2\pi\sigma^2\right) \\ & -\frac{1}{2\sigma^2}\sum_{k=1}^{K}\sum_{i=-N}^{N}\left(x_i(k)-\sum_{l=1}^{L} s_l(k)e^{j\omega_l k}e^{j(i\gamma_l+i^2\phi_l)}\right)^H \\ & \left(x_i(k)-\sum_{l=1}^{L} s_l(k)e^{j\omega_l k}e^{j(i\gamma_l+i^2\phi_l)}\right) \end{aligned} \tag{A4}$$

Based on (37), (38) and (39), the partial derivative respect to the three elements of ψ_l for the near-field or far-field sources can be respectively given by

$$\frac{\partial \ln(p(\mathbf{x}|\psi))}{\partial \omega_l} = \frac{1}{\sigma^2}\sum_{k=1}^{K}\sum_{i=-N}^{N}\left\{\mathrm{Re}\left(jks_l(k)e^{j\omega_l k}e^{j\left(i\gamma_l+i^2\phi_l\right)}n_i^*(k)\right)\right\}, \tag{A5}$$

$$\frac{\partial \ln(p(\mathbf{x}|\psi))}{\partial \theta_l} = \frac{1}{\sigma^2}\sum_{k=1}^{K}\sum_{i=-N}^{N}\left\{\mathrm{Re}\left[jks_l(k)e^{j\omega_l k}e^{j(i\gamma_l+i^2\phi_l)}\left(-\frac{2\pi di\cos\theta_l}{\lambda_l}-\frac{\pi d^2 i^2\sin(2\theta_l)}{\lambda_l r_l}\right)n_i^*(k)\right]\right\}, \tag{A6}$$

$$\frac{\partial \ln(p(\mathbf{x}|\psi))}{\partial r_l} = \frac{1}{\sigma^2}\sum_{k=1}^{K}\sum_{i=-N}^{N}\left\{\mathrm{Re}\left[jks_l(k)e^{j\omega_l k}e^{j(i\gamma_l+i^2\phi_l)}\left(-\frac{\pi d^2 i^2\cos^2\theta_l}{r_l^2}\right)n_i^*(k)\right]\right\} \tag{A7}$$

So the partial derivative with respect to ψ_l for the near-filed and far-field sources can be expressed as follows

$$\frac{\partial \ln(p(\mathbf{x}|\psi))}{\partial \psi_l} = \left[\frac{\partial \ln(p(\mathbf{x}|\psi))}{\partial \omega_l}\frac{\partial \ln(p(\mathbf{x}|\psi))}{\partial \theta_l}\frac{\partial \ln(p(\mathbf{x}|\psi))}{\partial r_l}\right]^T \tag{A8}$$

Based on (40)–(43), we obtain $\frac{\partial \ln(p(\mathbf{x}|\psi))}{\partial \psi_l}$ for all L sources and then form the following column vector $\frac{\partial \ln(p(\mathbf{x}|\psi))}{\partial \psi}$ by using $\frac{\partial \ln(p(\mathbf{x}|\psi))}{\partial \psi_l}$

$$\frac{\partial \ln(p(\mathbf{x}|\psi))}{\partial \psi} = \left[\frac{\partial \ln(p(\mathbf{x}|\psi))}{\partial \psi_1} \cdots \frac{\partial \ln(p(\mathbf{x}|\psi))}{\partial \psi_l} \cdots \frac{\partial \ln(p(\mathbf{x}|\psi))}{\partial \psi_L}\right]^T \tag{A9}$$

Based on (44), we obtain the Fisher information $\mathbf{F}$

$$\mathbf{F} = E\left[\frac{\partial \ln(p(\mathbf{x}|\psi))}{\partial \psi}\left(\frac{\partial \ln(p(\mathbf{x}|\psi))}{\partial \psi}\right)^T\right] \tag{A10}$$

So the CRB on the variance of the estimated parameters can be obtained from the related diagonal elements of the inverse $\mathbf{F}^{-1}$ [20]. In this paper, the Fisher information matrix $\mathbf{F}$ is estimated by averaging the 400 computations of $\frac{\partial \ln(p(\mathbf{x}|\psi))}{\partial \psi}(\frac{\partial \ln(p(\mathbf{x}|\psi))}{\partial \psi})^{\mathrm{T}}$ in the 400 independent Monte Carlo runs.

REFERENCES

1. Krim, H. and M. Viberg, "Two decades of array signal processing research: The parametric approach," *IEEE Transactions on Signal Processing Magazine*, Vol. 13, No. 4, 67–94, 1996.
2. Schmidt, R. O., "Multiple emitter location and signal parameter estimation," *IEEE Transactions on Antennas and Propagation*, Vol. 34, No. 3, 276–280, 1986.
3. Roy, R. and T. Kailath, "ESPRIT-estimation of signal parameters via rotational invariance techniques," *IEEE Transactions on Acoustics, Speech and Signal Processing*, Vol. 37, No. 7, 984–995, 1989.
4. Gao, F. and A. B. Gershman, "A generalized ESPRIT approach to direction-of-arrival estimation," *IEEE Signal Processing Letters*, Vol. 12, No. 3, 254–257, 2005.
5. Liu, F. L., J. K. Wang, and C. Y. Sun, "Spatial differencing method for DOA estimation under the coexistence of both uncorrelated and coherent signals," *IEEE Transactions on Antennas and Propagation*, Vol. 60, No. 4, 2052–2062, 2012.
6. Huang, Y. D. and M. Barkat, "Near-field multiple source localization by passive sensor array," *IEEE Transactions on Antennas and Propagation*, Vol. 39, No. 7, 968–975, 1991.
7. Chen, J. F. and X. L. Zhu, "A new algorithm for joint range-DOA-frequency estimation of near-field sources," *EURASIP Journal on Applied Signal Processing*, 386–392, 2004.
8. Zhi, W. and M. Y. M. Chia, "Near-field source localization via symmetric subarrays," *IEEE Signal Processing Letters*, Vol. 14, No. 6, 409–412, 2007.
9. Liang, J., X. Zeng, and B. Ji, "A computationally efficient algorithm for joint range-DOA-frequency estimation of near-field sources," *Digital Signal Processing*, Vol. 19, No. 4, 596–611, 2009.
10. Liang, J. and D. Liu, "Passive localization of mixed near-field and far-field sources using two-stage MUSIC algorithm," *IEEE Transactions on Signal Processing*, Vol. 58, No. 1, 108–120, 2010.
11. He, J., M. N. S. Swamy, and M. O. Ahmad, "Efficient application of MUSIC algorithm under the coexistence of far-field and near-field sources," *IEEE Transactions on Signal Processing*, Vol. 60, No. 4, 2066–2070, 2012.
12. Jiang, J. J., F. J. Duan, and J. Chen, "Mixed near-field and far-field sources localization using the uniform linear sensor array," *IEEE Sensors Journal*, Vol. 19, No. 8, 487–490, 2012.
13. Liu, G. H. and X. Y. Sun, "Two-stage matrix differencing algorithm for mixed far-field and near-field sources classification and localization," *IEEE Sensors Journal*, Vol. 14, No. 6, 1957–1965, 2014.
14. Du, R., F. Liu, and J. Wang, "Space-time matrix method for mixed near-field and far-field sources localization," *Progress In Electromagnetics Research M*, Vol. 36, 131–137, 2014.
15. Wang, B., J. Liu, and X. Y. Sun, "Mixed sources localization based on sparse signal reconstruction," *IEEE Signal Processing Letters*, Vol. 19, No. 8, 487–490, 2012.
16. Wang, B., Y. P. Zhao, and J. J. Liu, "Mixed-order MUSIC algorithm for localization of far-field and near-field sources," *IEEE Signal Processing Letters*, Vol. 20, No. 4, 311–314, 2013.
17. Jiang, J.-J., F.-J. Duan, and J. Chen, "Three-dimensional localization algorithm for mixed near-field and far-field sources based on ESPRIT and MUSIC method," *Progress In Electromagnetics Research*, Vol. 136, 435–456, 2013.

18. Swindlehurst, A. L. and T. Kailath, "Passive direction-of-arrival and range estimation for near-field sources," *IEEE Fourth Annual ASSP Workshop on Spectrum Estimation and Modeling*, 123–128, Minneapolis, MN, 1988.
19. Wax, M. and T. Kailath. "Detection of signals by information theoretic criteria," *IEEE Transaction on Acoustic, Speech, and Signal Processing*, Vol. 33, No. 2, 387–392, 1985.
20. Chen, Q., Y. B. Hua, and P. Stoica, "Asymptotic performance of optimal gain-and-phase estimators of sensor arrays," *IEEE Transactions on Signal Processing*, Vol. 48, No. 12, 3587–3590, 2000.
21. Wijnholds, S. J. and A. J. Veen, "Multisource self-calibration for sensor arrays," *IEEE Transactions on Signal Processing*, Vol. 57, No. 9, 3512–3522, 2009.
22. Wu, H. T., J. F. Yang, and F. K. Chen, "Source number estimators using transformed Gerschgorin radii," *IEEE Transactions on Signal Processing*, Vol. 43, No. 6, 1325–1333, 1995.
23. Kay, S. M., *Fundamentals of Statistical Signal Processing: Estimation Theory*, Prentice-Hall, New Jersey, 1993.